applied sciences

MDPI

Article

Exploration of Wendan Pomelo (*Citrus maxima* (Burm.) *Merr.* cv. *Wentan*) Peel from Four Different Growing Regions by Liquid Chromatography–Mass Spectrometry and Bioactivity Analysis

Jinlan Lu and Wenshu Wang *

College of Life and Environmental Sciences, Minzu University of China, Beijing 100081, China; zacklu400@foxmail.com

* Correspondence: wangws@muc.edu.cn; Tel.: +86-135-2296-5784

Abstract: Wendan (a type of pomelo), a popular fruit in China, is less known in other countries. Its peel is widely used in food and traditional medicine. Four different origins (Xuzhou, Taizhou, Zhangzhou, and Meizhou) of Wendan pomelo were selected, and crude extracts were obtained by the Soxhlet extraction method. The composition of Wendan peel was analyzed by high-performance liquid chromatography–mass spectrometry (HPLC-MS) in positive ion mode. The compounds were identified by searching the Metabolite Link (METLIN), the Spectral Database for Organic Compounds (SDBS), and by referring to literature reports. A total of 20 compounds were identified among the samples from the four origins, of which 8 compounds were common. The majority of the compounds belonged to the flavonoid and coumarin classes; Meranzin hydrate was identified for the first time in pomelo peel. In vitro antioxidant activity experiments showed that samples from Taizhou, Zhejiang, exhibited the highest antioxidant activity in the DPPH, ABTS, and FRAP assays, with values of 0.59 mg/mL, 97.06 μmol TE/g, and 60.62 μmol Fe^{2+}/g, respectively. Samples from Zhangzhou, Fujian, showed antioxidant activity second only to the samples from Taizhou, Zhejiang. The sample from Zhangzhou, Fujian Province, showed excellent inhibitory activity in the α-glucosidase inhibition assay (IC_{50} = 7.99 mg/mL).

Keywords: Wendan pomelo peel; chemical components; antioxidant; α-glucosidase

Citation: Lu, J.; Wang, W. Exploration of Wendan Pomelo (*Citrus maxima* (Burm.) *Merr.* cv. *Wentan*) Peel from Four Different Growing Regions by Liquid Chromatography–Mass Spectrometry and Bioactivity Analysis. *Appl. Sci.* **2024**, *14*, 1200. https://doi.org/10.3390/app14031200

Academic Editors: Natalija Velić and Olivera Galovic

Received: 10 December 2023
Revised: 28 January 2024
Accepted: 29 January 2024
Published: 31 January 2024

1. Introduction

Citrus maxima (Burm.) *Merr.*, commonly known as pomelo, is an evergreen tree belonging to the Rutaceae family. Its fruit has a smooth surface with small oil glands and is typically round or pear-shaped. The flesh of the fruit can be either white or red, with a few variants exhibiting a creamy yellow color. Pomelo cultivation can be found in various Southeast Asian regions such as Malaysia, Thailand, and Vietnam [1,2]. In China, it is primarily cultivated in Guangdong, Guangxi, Fujian, and Zhejiang [2].

Pomelo has been widely used in food and the cosmetic industry due to its special aroma, nutritional value, and pharmacological activity [3]. In China, pomelo is used traditionally as a functional food with the potential to balance insulin and glucose levels, thereby contributing to the management of diabetes [4]. Furthermore, pomelo products can be processed into pectin, essential oils, and dried pomelo peel [5]. In recent years, the industrial processing of pomelo products, such as beverages, canned foods, and wines, has been developing rapidly.

The pulp portion of pomelo is used as a fresh food to supplement nutrients such as vitamins. The peel, accounting for approximately 30% of the whole pomelo, is consumed directly in the form of sweets, tea, and medicine by locals on the southeast coast of China [2]. The bioactivities and phytochemistry of pomelo have been reviewed, including flavonoids, essential oils, coumarin classes, and triterpenes. Antioxidant, antibacterial, anticancer, and depression-alleviating properties were reported. For instance, naringin, hesperidin,

and neohesperidin showed remarkable antioxidant activity, indicating their potential as natural antioxidants. The flavonoid compounds demonstrated inhibitory effects against Escherichia coli, Pseudomonas aeruginosa, Bacillus subtilis, Staphylococcus aureus, Proteus mirabilis, and Vibrio anguillarum [6–9]. The antioxidant activity of pomelo peel was also reported. In previous studies, flavonoid (21.20 mg/100 g), vitamin C (15.13 mg/100 g), and carotenoid (62.98 μg/g) levels in an extract of pomelo peel were determined. The extract exhibited an IC50 value of 68.55 μg/mL by DPPH assay. This conclusion highlights the perspective that pomelo peel serves as a potential natural source of antioxidants [10]. However, there is relatively limited research on the classification of different species of pomelo.

The main pomelo species in China can be divided into three categories: Wendan pomelo, Shatian pomelo, and inter-specific pomelo [2]. Wendan pomelo is particularly well-known for its crisp and tender flesh, large size, and rich flavor. It was first cultivated in Zhangzhou, Fujian, and later introduced to other regions. Currently, the most famous Wendan pomelo species in China are Yuhuan Wendan from Taizhou, Zhejiang; Duwei Wendan from Putian, Fujian; and Madou Wendan from Tainan, Taiwan. With the widespread cultivation of Wendan pomelo, there was a continuous increase in its production. However, there is a lack of systematic research on Wendan pomelo peel, especially in terms of comparing the chemical composition and biological activities of Wendan pomelo peel from different cultivation regions.

Therefore, the present work investigated the composition and antioxidant activity of Wendan pomelo peel grown in China from four different origins.

2. Materials and Methods

2.1. Plant Materials

The Wendan (*Citrus maxima* cv. *Wentan Buntan*) peels were obtained from four different regions of China (Table 1, Figure 1): Xuzhou (Jiangsu), Taizhou (Zhejiang), Zhangzhou (Fujian), and Meizhou (Guangdong). The information used in the study also contained environmental factors such as latitude, longitude, temperature, precipitation, and humidity. These materials were identified by Professor Chun-lin Long (College of Life and Environmental Sciences, Minzu University of China) and *Flora of China*. The fresh Wendan peels were washed with distilled water, dried, and peeled. The Wendan pomelo peels were then placed in a cool and well-ventilated area for natural drying at a room temperature of approximately 25–30 °C while avoiding direct sunlight. After 2–3 weeks, the dried samples were collected, crushed, and stored in a cool place.

Table 1. Characteristics and information of samples.

Accessions Collected	Main Geographical Distribution	Longitude and Latitude	Traditional Name	Thickness of Peels (mm)	Precipitation [1] (mm)	Temperature [1] (°C)	Humidity [1] (%)
W1	Xuzhou, Jiangsu	N: 34°12′36″ E: 118°17′14″	Suqian mi you	1~2	801.3	16.4	72.2
W2	Taizhou, Zhejiang	N: 28°06′44″ E: 121°14′25″	Yuhuan wendan	2~3	1608.9	19.4	76.1
W3	Zhangzhou, Fujian	N: 24°25′22″ E: 117°28′16″	Pinghe you	2~3	1550.2	23.3	74.8
W4	Meizhou, Guangdong	N: 24°14′22″ E: 116°31′10″	Jiaxing mi you	1~2	1716.7	21.5	73.0

[1] The annual average meteorological data (2002–2022) of four locations from China Meteorological Data Service Center (CMDC, http://data.cma.cn/en) (CMDC, data.cma.cn, URL 12 October 2022).

The extractions were carried out by the Soxhlet extraction method. The ground peel of Wendan pomelo (6.0 g) was tightly wrapped in filter paper and placed into a Soxhlet extractor, which was then placed into a round-bottom flask (500 mL) containing 70% ethanol solution to obtain the extract. The extract was subjected to vacuum filtration with the addition of 25% ethanol solution for washing. The resulting filtrate was transferred to

a rotary evaporator and distilled under reduced pressure at 60 °C until no alcohol odor remained. Finally, the extract was dried in a fume hood.

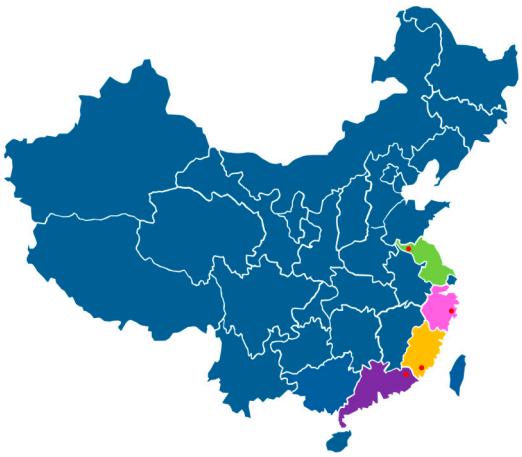

Figure 1. Jiangsu, Zhejiang, Fujian, and Guangdong Provinces are represented by the colors green, pink, orange, and purple, respectively. Sample collection sites are represented by the red dots.

2.2. HPLC-Q-TOF-MS/MS Analysis

The analysis [11] was conducted using the Agilent 1260 Infinity system (Agilent, Santa Clara, CA, USA) and the 1200 HPLC 6520 Q-TOF-MS (Agilent, Santa Clara, CA, USA). The samples were separated on a Hypersill Gold C18 column (250 mm × 4.6 mm, 5 µm, SN10609405, Thermo Scientific, Lenexa, KS, USA). The injection sample volume and flow rate were set at 2 µL and 1 mL/min, respectively. The gradient conditions were as follows: solvent A (H_2O-CH_2O_2, 1%) and solvent B (acetonitrile, C_2H_3N 99%). The initial setting was 0–5 min with a linear gradient of 10% B, followed by 5–35 min with 30% B, 35–45 min with 100% B, and then held at 10% B for 5 min to allow column equilibration. The detection range was set from 200 nm to 600 nm using nitrogen gas as the carrier. Mass spectrometry conditions included an electrospray ionization (ESI) source with an ion source temperature of 300 °C, positive ion detection, a scanning range of m/z 80–2000 Da, and a cone voltage of 30 V. Each batch of samples was tested in triplicate.

2.3. Nuclear Magnetic Resonance

^1H and ^{13}C NMR spectra (one-dimensional) were obtained on a Bruker Avance DRX-600 (Bruker, Berlin, Germany) spectrometer with a 5 mm TCI cryoprobe and a 14.1 T magnetic field. The chemical shifts of ^1H and ^{13}C were referenced according to the peak of the DMSO (C_2H_6OS) solvent used to solubilize the samples.

2.4. DPPH (2,2-Diphenyl-1-Picrylhydrazyl)-Assay

The DPPH free radical scavenging activity was assessed in accordance with a modified version of a known protocol [12]. The extract solutions were diluted with methanol to obtain a series of concentrations ranging from 10 to 500 µg/mL. The 0.06 mM DPPH solution was prepared by dissolving DPPH in methanol. The 100 µL aliquot of the sample was mixed with 100 µL of the DPPH solution and kept in the dark at room temperature. After 30 min, the absorbance of the solution was measured at 517 nm. BHT was used as a positive control, and methanol served as the blank control following the same experimental procedure. The radical scavenging activity was calculated using the equation as follows:

$$SC_{50}\ (\%) = [1 - (A_1 - A_2)/A_0] \times 100\%$$

where A_0 represents the absorbance of the blank control (methanol and DPPH solution), A_1 is the absorbance of the sample with DPPH solution, and A_2 is the absorbance of the

sample solution with methanol. The results were expressed as SC_{50} (mg/mL), and each batch of samples was tested in triplicate.

2.5. ABTS (2,2′-Azino-Bis (3-Ethylbenzothiazoline-6-Sulfonic Acid) Assay

The ABTS free radical scavenging activity was determined with slight modifications based on a previously described method [13]. The ABTS solution was prepared by mixing equal volumes of potassium persulfate (2.45 mM) and ABTS stock solution (7 mM) and allowing the mixture to react in the dark at room temperature for 12–16 h. The ABTS radical solution was then diluted with methanol to achieve an absorbance of 0.70 ± 0.02 at 734 nm. The Trolox ($C_{14}H_{18}O_4$) standard solution (10 mM) was prepared using methanol and further diluted with methanol to obtain a series of concentrations ranging from 0.1 to 0.7 mM. For the assay, 20 µL of Trolox was added to 180 µL of the ABTS solution and incubated in the dark at room temperature. After 10 min, the absorbance of the solution was measured at 734 nm. The same procedure was followed for the sample analysis. The standard curve was constructed using the Trolox standard solution with the absorbance as the ordinate and the Trolox concentration as the abscissa. The absorbance value obtained from the sample was then substituted into the standard curve to calculate the ABTS antioxidant activity. Each batch of samples was tested in triplicate, and the results were expressed as Trolox equivalent (µmol TE/g).

2.6. Ferric Reducing Antioxidant Power (FRAP) Assay

The FRAP assay was conducted with slight modifications based on a previously described method [14]. The working solution was prepared by combining 300 mM/L acetate buffer (pH 3.6), 10 mM/L TPTZ (tripyridyltriazine) solution in 40 mM/L HCl, and 20 mM/L $FeCl_3 \bullet 6H_2O$ solution in a volume ratio of 10:1:1. Prior to analysis, the FRAP solution was incubated in a 37 °C water bath. The samples were diluted with methanol, and 20 µL of the diluted sample solution was added to react with 180 µL of the FRAP solution at 37 °C in the dark. After 30 min, the absorbance at 593 nm was measured. A standard curve was constructed using the Fe^{2+} concentration as the abscissa and the absorbance as the ordinate to calculate the FRAP antioxidant activity. Each batch of samples was tested in triplicate, and the results were expressed as Fe^{2+} equivalent (µmol Fe^{2+}/g).

2.7. α-Glucosidase Inhibitory Assay

The α-glucosidase inhibitory assay was conducted with slight adjustments based on a previously described method [15]. The 1 U/mL α-glucosidase solution was prepared using phosphate buffer (0.1 M, pH 6.8). For the assay, 10 µL of the sample diluted in DMSO at various concentrations and 30 µL of α-glucosidase solution were mixed in 80 µL of potassium phosphate buffer and incubated for 5 min in a 37 °C water bath. Then, 30 µL of 20 mM PNPG (p-Nitrophenyl-β-D-G-alactopyranoside) was added to initiate the reaction, which was further incubated in a 37 °C water bath for 30 min. The reaction was terminated by adding 40 µL of Na_2CO_3 solution (2 M), and the absorbance was measured at 405 nm. Acarbose was used as a positive control. The inhibition ratio was calculated using the following equation:

$$\text{Inhibition (\%)} = [1 - (A_1 - A_0)/(A_3 - A_2)] \times 100\%$$

where A_0 represents the absorbance of the sample blank (phosphate buffer instead of PNPG), A_1 is the absorbance of the sample, A_2 is the absorbance of the control blank (phosphate buffer instead of the sample and PNPG), and A_3 is the absorbance of the control (phosphate buffer instead of the sample). The results were expressed as IC_{50} (mg/mL), and each batch of samples was tested in triplicate.

2.8. Statistical Analysis

For statistical analysis, the data obtained from this experiment were subjected to one-way analysis of variance (ANOVA) and Duncan tests. Each experiment was repeated three times, and the mean value was calculated. The results were presented as mean ± standard deviation (SD). Statistical analyses were performed using SPSS software (version 24, SPSS Inc., Chicago, IL, USA).

3. Results and Discussion

3.1. Identification Components of Wendan Pomelo Peel

The ion chromatograms in positive ion mode obtained by HPLC-MS/MS for the pericarp of four different origins of Wendan pomelo peel are shown in Figure 2. The chemical composition results are presented in Table 2. A total of 20 compounds (Figure 3) were detected in the samples from the four origins, with 8 compounds (chlorogenic acid (CP4), rutin (CP5), genipin-β-gentiobioside (CP9), narirutin (CP10), hesperidin (CP11), neohesperidin (CP12), meranzin hydrate (CP13), and isoquercitrin (CP18)) common to all four samples. A further two compounds were identified, but their names remain unknown. The major compounds were coumarins and flavonoids. The compound meranzin hydrate (CP13), which belongs to the coumarin compounds, exhibited the highest peak area in the chromatogram. This compound was first discovered in the root of Prangos ferulacea in 1972 [16] and is commonly studied in the context of Chaihu-Shugan-San [17]. It was the first time that this compound was discovered in Wendan pomelo peel. The flavonoid compounds with higher peak areas in the chromatogram were identified as rutin (CP5), narirutin (CP10), hesperidin (CP11), neohesperidin (CP12), and kaempferol (CP14). There were significant differences in peak areas among samples from different origins, with the proportions of coumarin compounds and flavonoid compounds in the Zhangzhou samples being similar, while the coumarins were much more abundant than the flavonoids in the samples from Xuzhou and Meizhou.

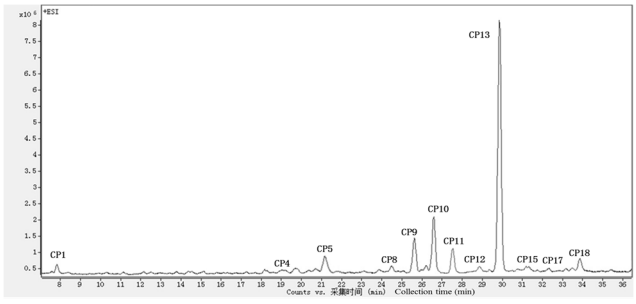

The ion chromatogram of W1

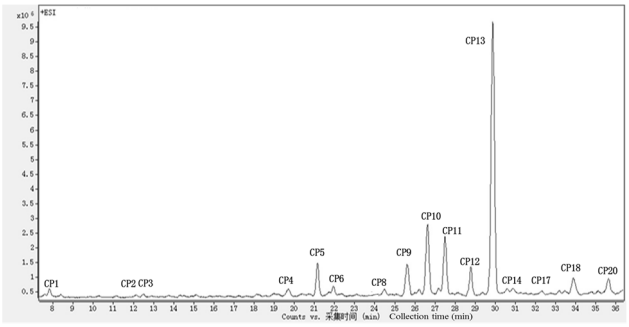

The ion chromatogram of W2

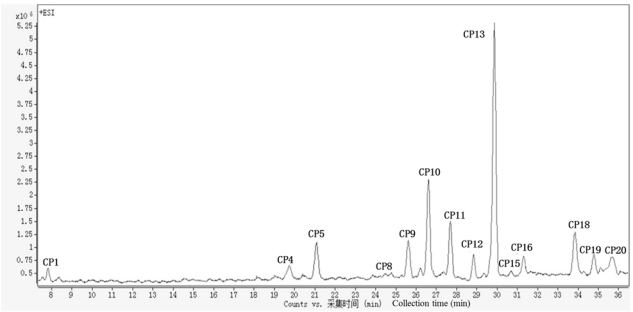

The ion chromatogram of W3

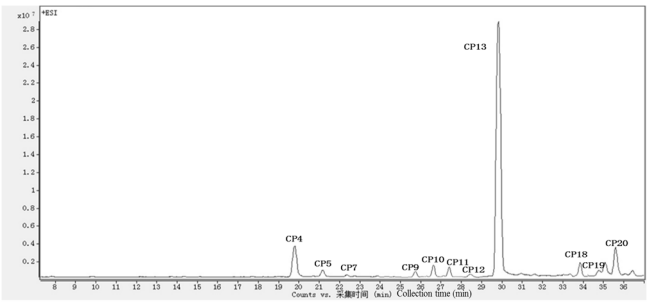

The ion chromatogram of W4

Figure 2. The ion chromatogram of Wendan pomelo peel from different regions.

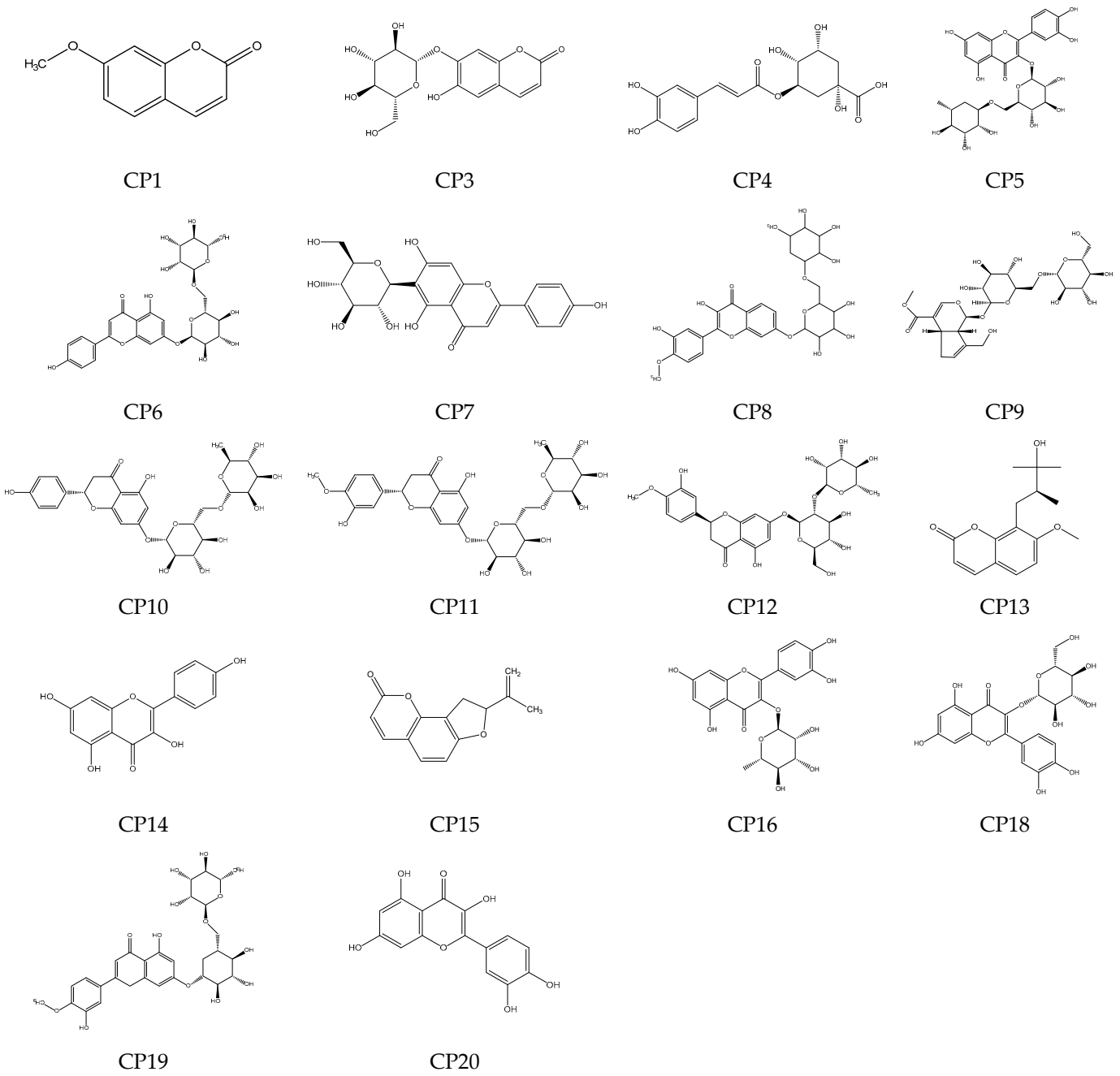

Figure 3. The structural formula of compounds.

Significant variations were observed in the chemical composition of samples from different origins. For instance, the sample from Zhejiang, Taizhou (W3), exhibited the highest number of detected compounds, with a total of 16 compounds. The sample from Guangdong, Meizhou (WF4), had the lowest number of detected compounds, with 11 compounds identified only. For these compounds, CP2, CP3, CP6, and CP16 were exclusively found in the sample from Taizhou, while CP14 was only detected in the sample from Zhangzhou, and CP15 was present solely in the sample from Xuzhou. Compound CP8 was not detected in the sample of Meizhou. Previous studies suggested that variations in plant chemical composition may be attributed to ecological differences [18,19]. Differences in chemical composition were observed in samples of the same plant species collected from different regions or even different locations within the same region, as described by Zhang et al. [20].

Table 2. The chemical constituents of Wendan pomelo peel from four areas.

Number [a]	Rt (min)	Molecular Formula	Fragments (*m*/*z*)			Compound	W1	W2	W3	W4
			1 [b]	2	3					
CP1	7.81	$C_{10}H_8O_3$	177.2405	133.1216	121.1081	7-methoxycoumarin *	+	+	+	-
CP2	12.13	$C_{15}H_{16}O_9$	341.2512	323.1103	305.0924	Unknown	-	+	-	-
CP3	12.52	$C_{15}H_{16}O_9$	341.0807	179.0340	151.0388	Esculetin-6-*O*-glucoside [c]	-	+	-	-
CP4	19.73	$C_{16}H_{18}O_9$	355.1029	163.0392	145.0287	Chlorogenic acid [c]	+	+	+	+
CP5	21.17	$C_{27}H_{30}O_{16}$	611.1611	465.1029	303.0501	Rutin *	+	+	+	+
CP6	21.95	$C_{27}H_{30}O_{14}$	579.1710	433.1132	271.0603	Apigenin-*O*-(deoxyhexosyl)hexoside [c]	-	+	-	-
CP7	22.31	$C_{21}H_{20}O_{10}$	433.1135	415.1034	397.0923	Isovitexin [c]	-	-	-	+
CP8	24.49	$C_{28}H_{32}O_{16}$	625.2113	607.1564	589.3071	Lucenin-2 4′-methylether [d]	+	+	+	-
CP9	25.61	$C_{23}H_{34}O_{15}$	573.1811	551.2143	227.1936	Genipin-*β*-gentiobioside [e]	+	+	+	+
CP10	26.68	$C_{27}H_{32}O_{14}$	581.1881	419.1349	273.0763	Narirutin *	+	+	+	+
CP11	27.55	$C_{28}H_{34}O_{15}$	611.1994	449.1457	303.0870	Hesperidin *	+	+	+	+
CP12	28.91	$C_{28}H_{34}O_{15}$	611.1987	449.1447	303.0871	Neohesperidin *	+	+	+	+
CP13	29.87	$C_{15}H_{18}O_5$	279.1243	261.1294	243.1027	Meranzin hydrate *,[x]	+	+	+	+
CP14	30.88	$C_{15}H_{10}O_6$	287.0553	258.0522	213.0543	Kaempferol *,[c]	-	+	+	-
CP15	31.14	$C_{11}H_6O_3$	187.0401	159.0444	143.0499	Angelicin [c]	+	-	-	-
CP16	31.36	$C_{21}H_{20}O_{11}$	449.1078	303.0501	229.0495	Quercitrin [c]	-	-	+	-
CP17	32.28	$C_{20}H_{24}O_{11}$	441.2495	352.3446	282.2769	Unknown	+	+	-	-
CP18	33.88	$C_{21}H_{20}O_{12}$	465.4033	303.2861	274.3367	Isoquercitrin *	+	+	+	+
CP19	34.83	$C_{28}H_{32}O_{15}$	609.1820	463.1244	301.1069	Diosmetin-7-*O*-rutinoside [c]	-	-	+	+
CP20	35.62	$C_{15}H_{10}O_7$	303.0507	285.0409	257.0453	Quercetin [c]	-	+	+	+

[a] Compound numbers are denoted as CPX (X = 1–20), [a b] represents the main fragment ion $[M+H]^+$, * indicates confirmation through standard compounds; "c–e" represents references [21–23]; [x] indicates determination through nuclear magnetic resonance analysis. "+" indicates the presence of the compound; "-" indicates the absence of the compound.

3.2. NMR

The compound CP13 was characterized based on the analysis of 1H NMR and 13C NMR spectra. In the ^{1}H NMR spectrum (Figure 4), methyl signals at δ 1.13 (s, H-17), 1.14 (s, H-18), and 3.87 (s, H-13) were observed on three carbon atoms. Additionally, four olefinic signals were detected at δ 6.24 (t, H-2), 7.95 (t, H-3), 7.53 (t, H-7), and 7.03 (t, H-8). Analysis of the ^{13}C NMR spectrum (Figure 5) revealed a total of 15 carbon atoms in the compound, including three signals of CH_3, one signal of CH_2, five signals of CH, and six signals of C. The ^{1}H NMR and ^{13}C NMR spectra displayed characteristic signals for a coumarin nucleus substituted on seven by a methoxyl group. The molecular formula of CP13 was determined as $C_{15}H_{18}O_5$ based on the results obtained from MS, in conjunction with the analysis of the ^{1}H NMR and ^{13}C NMR spectra. The compound was identified as a meranzin hydrate through structural elucidation. Meranzin hydrate was previously identified as a major constituent of the traditional Chinese medicine Chaihu-Shugan-San. In the reported studies, mice on a high-fat diet were subjected to gastric injections of high and low doses of Chaihu-Shugan-San and meranzin hydrate. Depressive-like behavior was evaluated through a sucrose preference test, open field test, light–dark test, and tail suspension test. The anti-atherosclerotic and anti-depressive properties of the compound meranzin hydrate were demonstrated by measuring arterial atherosclerotic plaques, blood lipid levels, and inflammatory cytokine levels [17]. In the four samples analyzed, this compound exhibited the highest proportion, indicating its significant research potential.

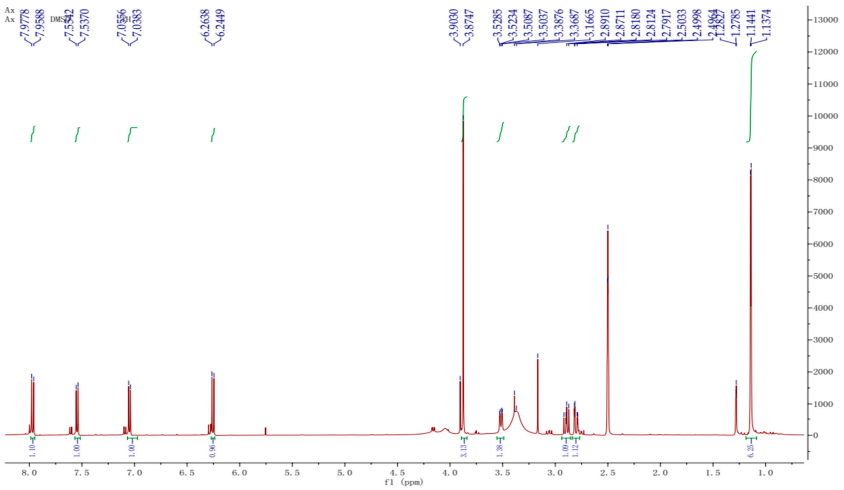

Figure 4. The ^{1}H NMR spectrum of meranzin hydrate.

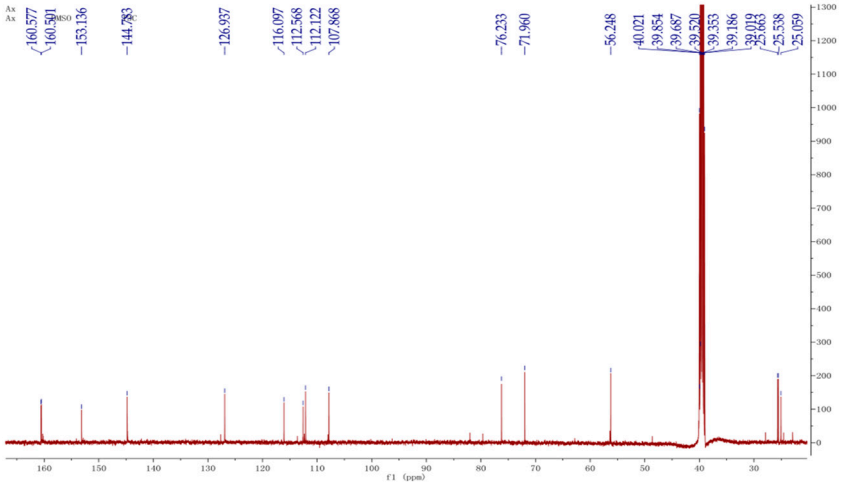

Figure 5. The ^{13}C NMR spectrum of meranzin hydrate.

3.3. Antioxidant Activities

The DPPH assay, as an in vitro antioxidant activity assessment, exhibits a lower value, indicating more significant antioxidant activity. The concentration of BHT corresponding to a 50% DPPH radical scavenging rate (SC_{50}) was found to be 0.11 mg/mL (Figure 6). The samples of W2 and W3 demonstrated values of 0.59 mg/mL and 1.75 mg/mL, respectively, indicating better antioxidant activity among samples. Additionally, the samples of W3 exhibited slightly lower antioxidant activity compared to the samples of W1. The samples of both W1 and W4 exhibited relatively weaker antioxidant capabilities, with SC_{50} values of 7.84 mg/mL and 5.96 mg/mL, respectively.

The ABTS and FRAP assay results were expressed in terms of Trolox equivalents and Fe^{2+} concentrations, respectively, where higher values indicate stronger antioxidant capacity. The samples of W2, according to Figure 7, exhibited the highest antioxidant capacity in both the ABTS and FRAP assays, with values of 97.06 μmol TE/g and 60.62 μmol Fe^{2+}/g, respectively. The W3 samples showed a slightly lower antioxidant capacity than W2 in the ABTS and FRAP assays, with values of 64.08 μmol TE/g and 45.29 μmol Fe^{2+}/g, respectively. However, the samples of W1 and W4 demonstrated relatively weaker antioxidant capacities; W1 displayed the weakest antioxidant activity in both tests.

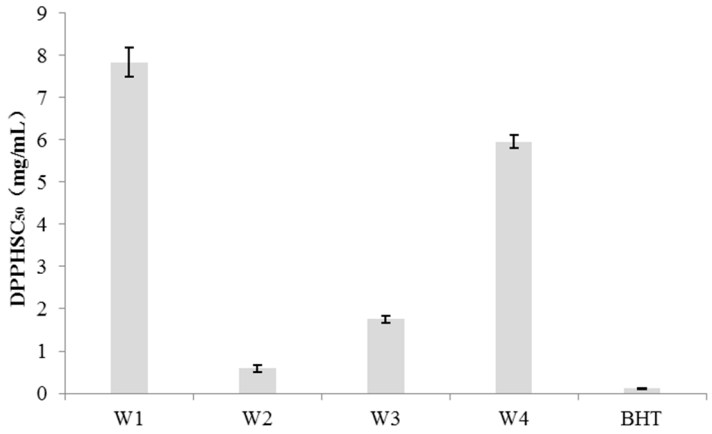

Figure 6. DPPH scavenging ability of samples from four regions.

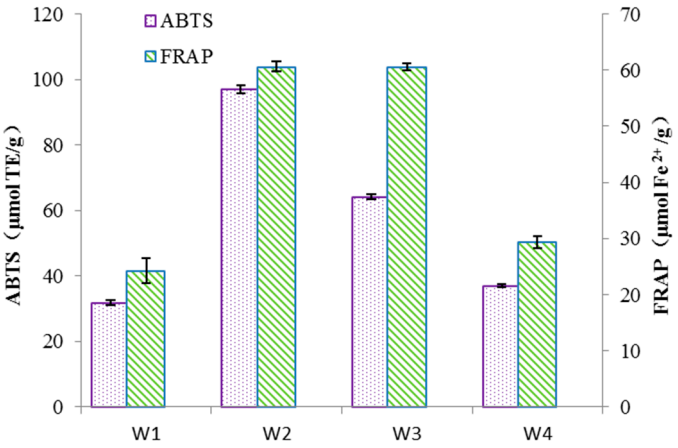

Figure 7. Antioxidant activities of samples from four regions in ABTS and FRAP assay.

Previous studies demonstrate the favorable antioxidant activity of flavonoid compounds in Citrus fruits [24]. Rutin (CP5), for instance, exerts its free radical scavenging effect through its ability to eliminate hydrogen peroxide and peroxides [25]. Naringin (CP10) exhibits strong antioxidant properties due to its ability to eliminate free radicals [26,27], while hesperidin (CP11) exerts antioxidant effects by attenuating oxidative stress reactions [28]. Neohesperidin (CP12) was also confirmed to possess excellent free radical scavenging abilities in both superoxide and hydroxyl radical tests [29]. These four compounds were detected in all the samples in this study, and in the absence of considering compound synergistic effects, these four compounds provide a relevant explanation for the observed antioxidant activity. However, the compound kaempferol (CP14) was shown to possess antioxidant activity [30]. Considering the differences in compound composition among samples and the potential synergistic effects between compounds [31], this may explain why the samples of W2 and W3 exhibited stronger antioxidant capacity, while the samples of W1 and W4 showed relatively weaker activity.

3.4. α-Glucosidase Inhibitory Activity

The α-glucosidase inhibition activity, according to Table 3, was evaluated as a measure of hypoglycemia, with lower values indicating stronger blood glucose-lowering ability. All samples from the four regions exhibited weaker activity compared to the positive control acarbose, but the samples of W3 (I = 7.99 mg/mL) demonstrated the highest inhibitory activity of all samples, followed by W1 with a value of 11.86 mg/mL. Samples of W2 showed moderate activity with a value of 12.38 mg/mL, while W4 exhibited the weakest inhibitory activity.

Table 3. The α-Glucosidase inhibitory activities of samples from four regions.

Sample	*I* (mg/mL)
WF1	11.86 ± 0.40
WF2	12.38 ± 1.33
WF3	7.99 ± 0.83
WF4	15.6 ± 0.35
acarbose	0.96 ± 0.07

Previous research demonstrated the potential benefits of rutin (CP5) in managing hypertension, hyperlipidemia, and hyperglycemia [32]. Both naringin (CP10) and hesperidin (CP11) were found to reduce blood glucose levels by inhibiting stress responses induced by glucose [33]. Moreover, hesperidin (CP11) has the ability to mitigate oxidative stress through the enhancement of kinase activity, thereby contributing to its hypoglycemic effects [34]. These three compounds were detected in all samples, providing a comprehensive explanation for the observed α-glucosidase inhibitory activity. The α-glucosidase inhibitory activity cannot be solely attributed to rutin, naringin, and hesperidin, as it may also be related to other compounds. For instance, studies indicated that quercitrin exhibits significant inhibitory effects on α-amylase and α-glucosidase, making it an ideal compound for targeting diabetes management [35,36]. Based on the obtained chemical composition, and without considering synergistic effects, it was observed that the compound quercitrin (CP16) detected in samples of W3 was not found in other samples. Therefore, the presence of quercitrin in samples of W3 may serve as a crucial indicator of its superior inhibitory activity compared to other samples. Additional research is warranted to explore the interactions between various compounds and the potential synergistic effects that may arise from these interactions.

4. Conclusions

This study compared the chemical composition and biological activities of Wendan peel samples collected from four different regions in China. The results revealed variations in the chemical composition of the samples from four different origins. A total of 20 compounds, primarily flavonoids and coumarins, were detected among the four samples. Eight compounds were found to be common among the samples, with meranzin hydrate, rutin, narirutin, hesperidin, neohesperidin, and kaempferol being the major compounds with larger peak areas. Furthermore, significant differences were observed in the chemical composition and bioactivity of the samples from different regions. The bioactivity assays demonstrated that the sample from Taizhou (W2) exhibited the highest antioxidant activity, followed by the sample from Zhangzhou (W3). These two samples could be considered potential natural antioxidants. Additionally, the sample from Zhangzhou (W3) could be regarded as a promising source for the research and development of natural α-glucosidase inhibitors. Based on the experimental results, it can be inferred that precipitation within the range of 1500–1600 mm, temperature between 19 and 23 °C, and humidity of 74–76% contribute to the formation and accumulation of compounds. This might explain why the samples from Taizhou, Zhejiang (W2), and Zhangzhou, Fujian (W3), demonstrated favorable data. From the perspective of future research value, Taizhou, Zhejiang, and Zhangzhou, Fujian, can be regarded as the optimal cultivation regions for Wendan pomelo.

Author Contributions: Conceptualization, J.L.; methodology, J.L.; data curation, J.L.; writing—original draft preparation, J.L.; writing—review and editing, J.L. and W.W. All authors have read and agreed to the published version of the manuscript.

Funding: This research received no external funding.

Institutional Review Board Statement: Not applicable.

Informed Consent Statement: Not applicable.

Data Availability Statement: The data presented in this study are available in article.

Acknowledgments: We would like to acknowledge the technical guidance provided by the Institute of Microbiology, Chinese Academy of Sciences.

Conflicts of Interest: The authors declare no conflicts of interest.

References

1. Burana-Osot, J.; Soonthornchareonnon, N.; Chaidedgumjorn, A.; Hosoyama, S.; Toida, T. Determination of galacturonic acid from pomelo pectin in term of galactose by hpaec with fluorescence detection. *Carbohydr. Polym.* **2010**, *81*, 461–465. [CrossRef]
2. Editorial Committee of the Flora of China, Chinese Academy of Sciences. *Flora of China Volume 1 to Volume 65*; Science Press: Beijing, China, 1997; Volume 43, pp. 13–17.
3. Jiang, L.Y. Study on the Antibacterial Activity of the Extract from Peel of Pomelo. *J. Anhui Agric. Sci.* **2008**, *36*, 9354–9355. [CrossRef]
4. Murunga, A.N.; Miruka, D.O.; Driver, C.; Nkomo, F.S.; Cobongela, S.Z.; Owira, P.M. Grapefruit derived flavonoid naringin improves ketoacidosis and lipid peroxidation in type 1 diabetes rat model. *PLoS ONE* **2016**, *11*, e0153241. [CrossRef]
5. Huyen, L.T.; On, T.N.H.; Nhi, T.T.; Phat, D.T.; Cang, M.H. Product diversification from pomelo peel. Essential oil, Pectin and semi-dried pomelo peel. *Pol. J. Chem. Technol.* **2021**, *23*, 17–25. [CrossRef]
6. Wu, T.; Guan, Y.; Ye, J. Determination of flavonoids and ascorbic acid in grapefruit peel and juice by capillary electrophoresis with electrochemical detection. *Food Chem.* **2007**, *100*, 1573–1579. [CrossRef]
7. Njoroge, S.M.; Koaze, H.; Karanja, P.N.; Sawamura, M. Volatile constituents of redblush grapefruit (*Citrus paradisi*) and pummelo (*Citrus grandis*) peel essential oils from Kenya. *J. Agric. Food Chem.* **2005**, *53*, 9790–9794. [CrossRef]
8. Xi, W.; Fang, B.; Zhao, Q.; Jiao, B.; Zhou, Z. Flavonoid composition and antioxidant activities of Chinese local pummelo (*Citrus grandis* Osbeck.) varieties. *Food Chem.* **2014**, *161*, 230–238. [CrossRef]
9. Li, X.; Ye, F.; Zhou, Y.; Zhao, G.; Zhao, G. Utilization of pomelo peels to manufacture value-added products: A review. *Food Chem.* **2021**, *351*, 129247. [CrossRef]
10. Abudayeh, Z.H.; Al Khalifa, I.I.; Mohammed, S.M.; Ahmad, A.A. Phytochemical content and antioxidant activities of pomelo peel extract. *Pharmacogn. Res.* **2019**, *11*, 244. [CrossRef]
11. Dugo, P.; Mondello, L.; Morabito, D.; Dugo, G. Characterization of the Anthocyanin Fraction of Sicilian Blood Orange Juice by Micro-HPLC-ESI/MS. *J. Agric. Food Chem.* **2003**, *51*, 1173–1176. [CrossRef]
12. Hatano, T.; Edamatsu, R.; Hiramatsu, M.; Mori, A.; Fujita, Y.; Yasuhara, T.; Yoshida, T.; Okuda, T. Effects of the interaction of tannins with co-existing substances. VI. Effects of tannins and related polyphenols on superoxide anion radical and on 1, 1-diphenyl-2-picrylhydrazyl radical. *Chem. Pharm. Bull.* **2008**, *37*, 2016–2021. [CrossRef]
13. Cai, Y.; Luo, Q.; Sun, M.; Corke, H. Antioxidant activity and phenolic compounds of 112 traditional Chinese medicinal plants associated with anticancer. *Life Sci.* **2004**, *74*, 2157–2184. [CrossRef] [PubMed]
14. Benzie, I.F.F.; Strain, J.J. The Ferric Reducing Ability of Plasma (FRAP) as a Measure of "Antioxidant Power": The FRAP Assay. *Anal. Biochem.* **1996**, *239*, 70–76. [CrossRef] [PubMed]
15. Apostolidis, E.; Lee, C.M. In vitro potential of *Ascophyllum nodosum* phenolic antioxidant-mediated α-glycosidase and α-amylase inhibition. *J. Food Sci.* **2010**, *75*, H97–H102. [CrossRef] [PubMed]
16. Abyshev, A.Z.; Denisenko, P.P.; Kostyuchenko, N.P.; Ermakov, A.I.; Sheinker, Y.N. Natural meranzin hydrate-A new component of the roots of *Prangos ferulacea*. *Chem. Nat. Compd.* **1972**, *8*, 577–580. [CrossRef]
17. Li, L.; Yu, A.L.; Wang, Z.L.; Chen, K.; Zheng, W.; Zhou, J.J.; Xie, Q.; Yan, H.B.; Ren, P.; Huang, X. Chaihu-Shugan-San and absorbed meranzin hydrate induce anti-atherosclerosis and behavioral improvements in high-fat diet ApoE-/-mice via anti-inflammatory and BDNF-TrkB pathway. *Biomed. Pharmacother.* **2019**, *115*, 108893. [CrossRef] [PubMed]
18. Santos, C.P.D.; Pinto, J.A.O.; Santos, C.A.D.; Arie, F.B. Harvest time and geographical origin affect the essential oil of *Lippia gracilis* Schauer. *Ind. Crops Prod.* **2016**, *79*, 205–210. [CrossRef]
19. Delfine, S.; Marrelli, M.; Conforti, F.; Formisano, C.; Rigano, D.; Menichini, F. Variation of Malva sylvestris, essential oil yield, chemical composition and biologicalactivity in response to different environments across Southern Italy. *Ind. Crops Prod.* **2017**, *98*, 29–37. [CrossRef]
20. Zhang, L.; Yang, Z.; Chen, F.; Su, P.; Chen, D.; Pan, W.; Fang, Y.; Dong, C.; Zheng, X.; Du, Z. Composition and bioactivity assessment of essential oils of *Curcuma longa* L. collected in China. *Ind. Crops Prod.* **2017**, *109*, 60–73. [CrossRef]
21. Zengin, G.; Paksoy, M.Y.; Aumeeruddy, M.Z.; Glamocilja, J.; Sokovic, M.; Diuzheva, A.; Jeko, J.; Cziaky, Z.; Rodrigues, M.J.; Custodio, L.; et al. New insights into the chemical profiling, cytotoxicity and bioactivity of four *Bunium* species. *Food Res. Int.* **2019**, *123*, 414–424. [CrossRef]
22. Barreca, D.; Bellocco, E.; Leuzzi, U.; Gattuso, G. First evidence of C-and O-glycosyl flavone in blood orange (*Citrus sinensis* (L.) Osbeck) juice and their influence on antioxidant properties. *Food Chem.* **2014**, *149*, 244–252. [CrossRef]
23. Wu, H.; Li, X.; Yan, X.; An, L.; Luo, K.; Shao, M.; Jiang, Y.; Xie, R.; Feng, F. An untargeted metabolomics-driven approach based on LC–TOF/MS and LC–MS/MS for the screening of xenobiotics and metabolites of Zhi-Zi-Da-Huang decoction in rat plasma. *J. Pharm. Biomed. Anal.* **2015**, *115*, 315–322. [CrossRef] [PubMed]

24. Huang, R.; Zhang, Y.; Shen, S.; Zhi, Z.; Cheng, H.; Chen, S.; Ye, X. Antioxidant and pancreatic lipase inhibitory effects of flavonoids from different citrus peel extracts: An in vitro study. *Food Chem.* **2020**, *326*, 126785. [CrossRef] [PubMed]
25. Alam, P.; Alajmi, M.F.; Arbab, A.H.; Parvez, M.K.; Siddiqui, N.A.; Alqasoumi, S.I.; AI-Rehaily, A.J.; AI-Dosari, M.S.; Basudan, O.A. Comparative study of antioxidant activity and validated RP-HPTLC analysis of rutin in the leaves of different Acacia species grown in Saudi Arabia. *Saudi Pharm. J.* **2017**, *25*, 715–723. [CrossRef] [PubMed]
26. Safari, M.R.; Sheikh, N. Effects of flavonoids on the susceptibility of low-density lipoprotein to oxidative modification. *Prostaglandins Leukot. Essent. Fat. Acids* **2003**, *69*, 73–77. [CrossRef] [PubMed]
27. El-Desoky, A.H.; Abdel-Rahman, R.F.; Ahmed, O.K.; El-Beltagi, H.S.; Hattori, M. Anti-inflammatory and antioxidant activities of naringin isolated from Carissa carandas L.: In vitro and in vivo evidence. *Phytomedicine* **2018**, *42*, 126–134. [CrossRef] [PubMed]
28. Tirkey, N.; Pilkhwal, S.; Kuhad, A.; Chopra, K. Hesperidin, a citrus bioflavonoid, decreases the oxidative stress produced by carbon tetrachloride in rat liver and kidney. *BMC Pharmacol.* **2005**, *5*, 2. [CrossRef]
29. Suarez, J.; Herrera, M.D.; Marhuenda, E. In vitro scavenger and antioxidant properties of hesperidin and neohesperidin dihydrochalcone. *Phytomedicine* **1998**, *5*, 469–473. [CrossRef] [PubMed]
30. Tian, C.; Liu, X.; Chang, Y.; Wang, R.; Lv, T.; Cui, C.; Liu, M. Investigation of the anti-inflammatory and antioxidant activities of luteolin, kaempferol, apigenin and quercetin. *S. Afr. J. Bot.* **2021**, *137*, 257–264. [CrossRef]
31. Anagnostopoulou, M.A.; Kefalas, P.; Papageorgiou, V.P.; Assimopoulou, A.N.; Boskou, D. Radical scavenging activity of various extracts and fractions of sweet orange peel (*Citrus sinensis*). *Food Chem.* **2006**, *94*, 19–25. [CrossRef]
32. Kim, H.S. Effects of the Feral Peach (*Prunus persica Batsch* var. *davidiana* Max) Extract on the Lipid Compositions and Blood Pressure Level in Spontaneously Hypertensive Rats. *J. Life Sci.* **2006**, *16*, 1071–1079. [CrossRef]
33. Mahmoud, A.M.; Ashour, M.B.; Abdel-Moneim, A.; Ahmed, O.M. Hesperidin and naringin attenuate hyperglycemia-mediated oxidative stress and proinflammatory cytokine production in high fat fed/streptozotocin-induced type 2 diabetic rats. *J. Diabetes Complicat.* **2012**, *26*, 483–490. [CrossRef] [PubMed]
34. Yamamoto, M.; Suzuki, A.; Jokura, H.; Yamamoto, N.; Hase, T. Glucosyl hesperidin prevents endothelial dysfunction and oxidative stress in spontaneously hypertensive rats. *Nutrition* **2008**, *24*, 470–476. [CrossRef] [PubMed]
35. Van, L.V.; Pham, E.C.; Nguyen, C.V.; Duong, N.T.N.; Le Thi, T.V.; Truong, T.N. In vitro and in vivo antidiabetic activity, isolation of flavonoids, and in silico molecular docking of stem extract of *Merremia tridentata* (L.). *Biomed. Pharmacother.* **2022**, *146*, 112611. [CrossRef]
36. Oh, T.W.; Do, H.J.; Jeon, J.H.; Kim, K. Quercitrin inhibits platelet activation in arterial thrombosis. *Phytomedicine* **2021**, *80*, 153363. [CrossRef]